



Abstract

# Geochemical changes in mine tailings during a transition to pressure–oxidation process discharge, Macraes mine, New Zealand

D. Craw\*

*Geology Department and Environmental Science Programme, University of Otago, P.O. Box 56, Leith Street, Dunedin 9001, New Zealand*

Received 19 June 2002; accepted 7 April 2003

---

## Abstract

The Macraes gold mine, in southern New Zealand, was developed in a low grade mesothermal deposit. A pressure–oxidation plant was commissioned in 1999 to oxidize pyrite and arsenopyrite in the ore and release gold from within the sulphide grains. Pressure–oxidation discharges include anhydrite, jarosite, and amorphous Fe arsenates with molar Fe/As of 2–7 and up to 0.5 mol% S. Discharge waters contain dissolved Fe(II). There were profound chemical changes within the mine tailings system over the transition to pressure–oxidation. Dissolved sulphate of tailing waters increased to ca. 4000 mg/l, and the waters rapidly became saturated with respect to gypsum. Gypsum was precipitated in many parts of the water pathways at the plant and an estimated 1–4 tonnes of gypsum/day was precipitated in the tailings of the dam structure. The pH of tailings lowered from >8 to 6 with pressure–oxidation, but then evolved towards 8 again. The observed pH was a result of two opposing chemical processes: acidification due to oxidation of dissolved Fe(II) and dissolution of calcite. Calcite forms ca. 5 wt.% of tailings and is sufficiently abundant to dominate the chemistry of tailings. Dissolved arsenic in waters of tailings decreased from >10 to <<1 ppm after pressure–oxidation began, because the amorphous Fe arsenates are less soluble than arsenopyrite. Adsorption of dissolved As onto Fe(III) oxyhydroxides is effective in the tailings system, and strongly limits As discharge. Any As discharge will move through the tailings of the dam system at <30 mm/year.

© 2003 Elsevier Science B.V. All rights reserved.

*Keywords:* Mine tailings; New Zealand; Arsenic; Arsenate; pH; Geochemistry; Pressure oxidation

---

## 1. Introduction

Modern gold mines discharge voluminous tailings that formed as an essential part of the process of extracting small amounts of gold from large volumes of rock, typically <10 g Au/tonne of rock. Tailings are generally impounded behind large dams, and when

mining ceases, these impoundments are capped, revegetated, and left as permanent features on the landscape (Ritcey, 1989). Because the tailing impoundments are long-term repositories, the chemical processes occurring within them are of environmental significance because they govern the chemistry of the discharges from the impoundments. Once the tailings have been capped, it becomes difficult to infer the nature of these internal chemical processes. Studies of processes occurring in tailing impoundments before

---

\* Tel.: +64-3-4797519; fax: +64-3-4797527.

E-mail address: [dave.craw@stonebow.otago.ac.nz](mailto:dave.craw@stonebow.otago.ac.nz) (D. Craw).

they are capped provide a useful basis for predictions of longer-term chemical stability.

Pressure–oxidation technology has been developing over the past 10 years and this technology is becoming widely used in mineral processing. The principal reason for using this technology is to increase the proportion of gold extracted from the ore, in ores that are otherwise refractory. The oxidation process decomposes sulphides which commonly contain sub-microscopic and/or solid solution gold, and this gold then becomes accessible to cyanide solutions. Pressure–oxidation has profound effects on the mineralogy of the ore, and therefore the mineralogy of the material discharged into tailing impoundments. Consequently, the chemical processes occurring in impoundments containing tailings from pressure–oxidation plants are very different from those occurring in traditional sulphide-bearing tailings.

This study describes the chemical changes which occurred in a mine tailing impoundment during a transition from traditional carbon-in-pulp cyanidation (CIL) to pressure–oxidation treatment coupled with

cyanidation. Changes to water chemistry in the tailings over this transition are examined in the context of changes to ore and tailings mineralogy. From these observations, attempts are made to predict future changes within the tailings, for at least the short and medium term. The principal issues are acid generation, acid neutralisation, and arsenic mobility, and these are addressed in detail in the paper.

## 2. Macraes mine and processing plant

The Macraes mine extracts gold from a schist-hosted mesothermal gold vein deposit in southern New Zealand (McKeag et al., 1989; Craw et al., 1999, 2002). Gold occurs in close association with pyrite and arsenopyrite, which make up about 1% of the ore. The sulphides are concentrated about 10-fold by flotation after initial crushing. The mine opened in 1989 with carbon-in-pulp cyanidation (CIL), and this was augmented in 1999 with a pressure–oxidation step before cyanidation. The present processing plant

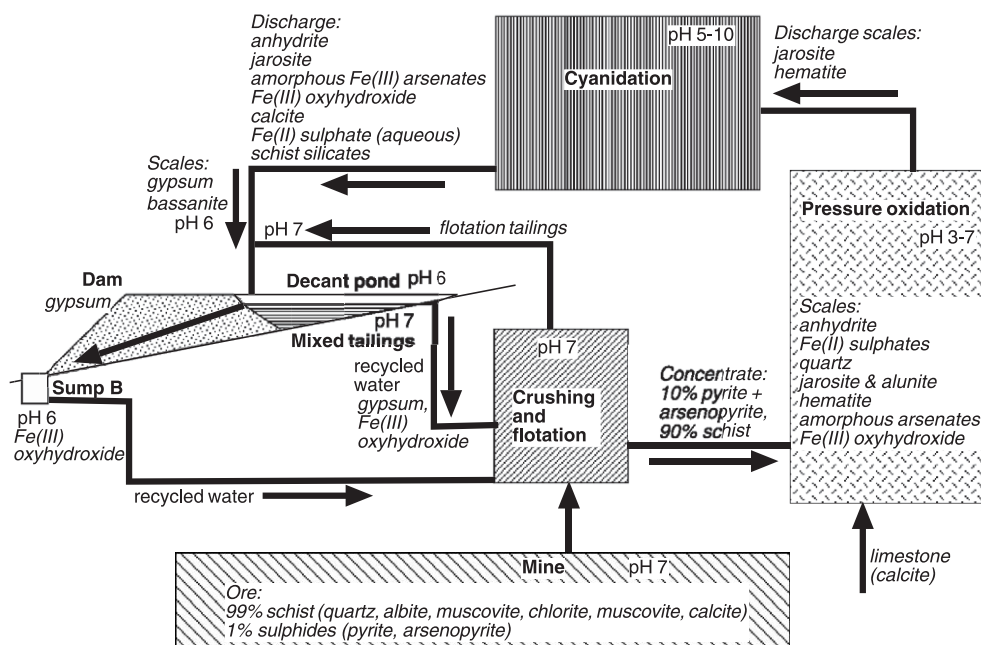


Fig. 1. Summary diagram of the Macraes mine processing system showing the principal features mentioned in this report. Idealised fluid pathways between stages in the processing system are shown with flow directions (large black arrows). Minerals indicated along the pathways are those which are input at various sites, and new minerals which form at each stage. Approximate pH values are indicated to show general plant-wide variations.

is complex in detail, but a summary is presented as Fig. 1 to show the setting of the pressure–oxidation part of the system (right hand side of diagram) in the context of the rest of the processing plant. Most of this paper focuses on the tailings system (left centre, Fig. 1), but some minor references are made to other stages in the plant.

The pressure–oxidation system centres on the autoclave, a large vessel in which the ore sulphide concentrate is oxidized at 225 °C under pressure with high-oxygen atmosphere. Sulphide oxidation results in acidification, which is partially neutralised with limestone added with the ore feed. Mineral precipitates, or scales, are left on the walls of the autoclave and slurry pipelines downstream of the autoclave. These minerals, identified by X-ray diffraction (XRD), give some indication of the nature of the chemical system at each step. Principal scale and discharge minerals are listed at various key points in the plant system in Fig. 1.

When the pressure–oxidation discharge material has passed through the cyanidation (CIL) tanks, it is mixed with tailings from the flotation stage before being discharged to the tailings impoundment. Flotation tailings consist almost entirely of schist host rock (predominantly quartz, albite, muscovite, chlorite, and calcite). The mixed tailing impoundment depicted in Fig. 1 received tailings from 1991 to early 2002. From early 2002, tailings were deposited in an exhausted mine open pit excavation, and the mixed tailings impoundment became inactive.

### 3. Autoclave minerals

A wide variety of minerals forms as scale up to 5 cm thick on the walls of the autoclave, with individual crystals up to 10 mm long. The crystalline material has been identified by XRD, and amorphous material partially characterized by electron microprobe. The mineral suite is dominated by anhydrite, Fe(II) sulphates, quartz, jarosite, alunite, hematite, and amorphous arsenates (Fig. 1). Autoclave discharge pipes have scales of jarosite and hematite (Fig. 1).

Solid discharge material from the autoclave was collected as CIL tailings before these are mixed with the flotation tailings. The autoclave discharge material is a fine-grained brown powder when dried. XRD analysis of the material shows that the powder is

dominated by anhydrite and muscovite, and no other identifiable minerals can be discerned from the XRD spectrum because of the dominance of these two minerals. About 1 g of effluent powder was mounted in epoxy resin and polished for examination by microprobe. Based on microprobe chemistry and knowledge of the autoclave system (above; Fig. 1), calcite and jarosite have been further identified in the brown powder. In addition, an orange brown iron-rich compound presumed to be a ferric oxide or hydroxide is a common component. This material is a less-crystalline form of the abundant hematite found as scale in the autoclave, and is referred to herein as Fe(III) oxyhydroxide. Similar brown iron-rich material contains abundant arsenic, and is presumed to be Fe arsenate related to the arsenate material found as scale in the autoclave (Fig. 1). This Fe arsenate material could be, at least in part, Fe(III) oxyhydroxide with variable amounts of admixed or adsorbed arsenic, but the optical appearance (next paragraph) implies that the material is a distinct phase or group of phases.

The Fe arsenate makes up about 20% of the discharge material, and should be discernable in XRD spectra if it is crystalline. Since it is not apparent in the XRD spectra, it is assumed to be amorphous. This amorphous Fe arsenate forms angular equant grains that range in size from 10 µm to less than 1 µm across. Smaller grains are locally clustered into larger composite particles, forming irregular masses. Some such masses coat other particles such as anhydrite and muscovite. Anhydrite grains are also generally irregular, and form most of the background mass of material. However, numerous fully or partly formed anhydrite crystals also occur. Some crystals amalgamate into star-shaped clusters, while elsewhere, anhydrite coats muscovite and Fe arsenate grains. There are two distinct types of Fe arsenate: one which has little sulphur, and one which has significant sulphur content. Semiquantitative microprobe analyses show a wide range in both molar Fe/As ratio (2–7) and in sulphur content (0.04 to 0.5 mol% S). None of the Fe arsenate discharged from the autoclave is scorodite (FeAsO<sub>4</sub>·2H<sub>2</sub>O).

Additional minerals that have been identified by microprobe in the fine grained discharge material are muscovite, quartz, chlorite, and feldspar, all of which were in the ore feed. The calcite which appears in the discharge material (above) may be from the ore feed or from the limestone added separately (Fig. 1).

#### 4. Decant pond water

Slurry from the CIL plant, containing the brown pressure–oxidation discharge material, was discharged into the mixed tailings impoundment with the flotation tailings (Fig. 1). This slurry was normally combined with the flotation tailings before discharge. Hence, the discharged material was grey with the brown pressure–oxidation effluent distrib-

uted evenly and strongly diluted. The sand/silt/mud suspended load settled rapidly in the mixed tailings impoundment to form layers of water-rich (ca. 50 vol%) sediment, and the rest of the water rose and coalesced into a broad shallow decant pond (Fig. 1). The decant water appears clear in sample bottles, but had a pale brown tinge when viewed from a distance in situ. The decant water was almost constantly recycled back to the processing plant and therefore

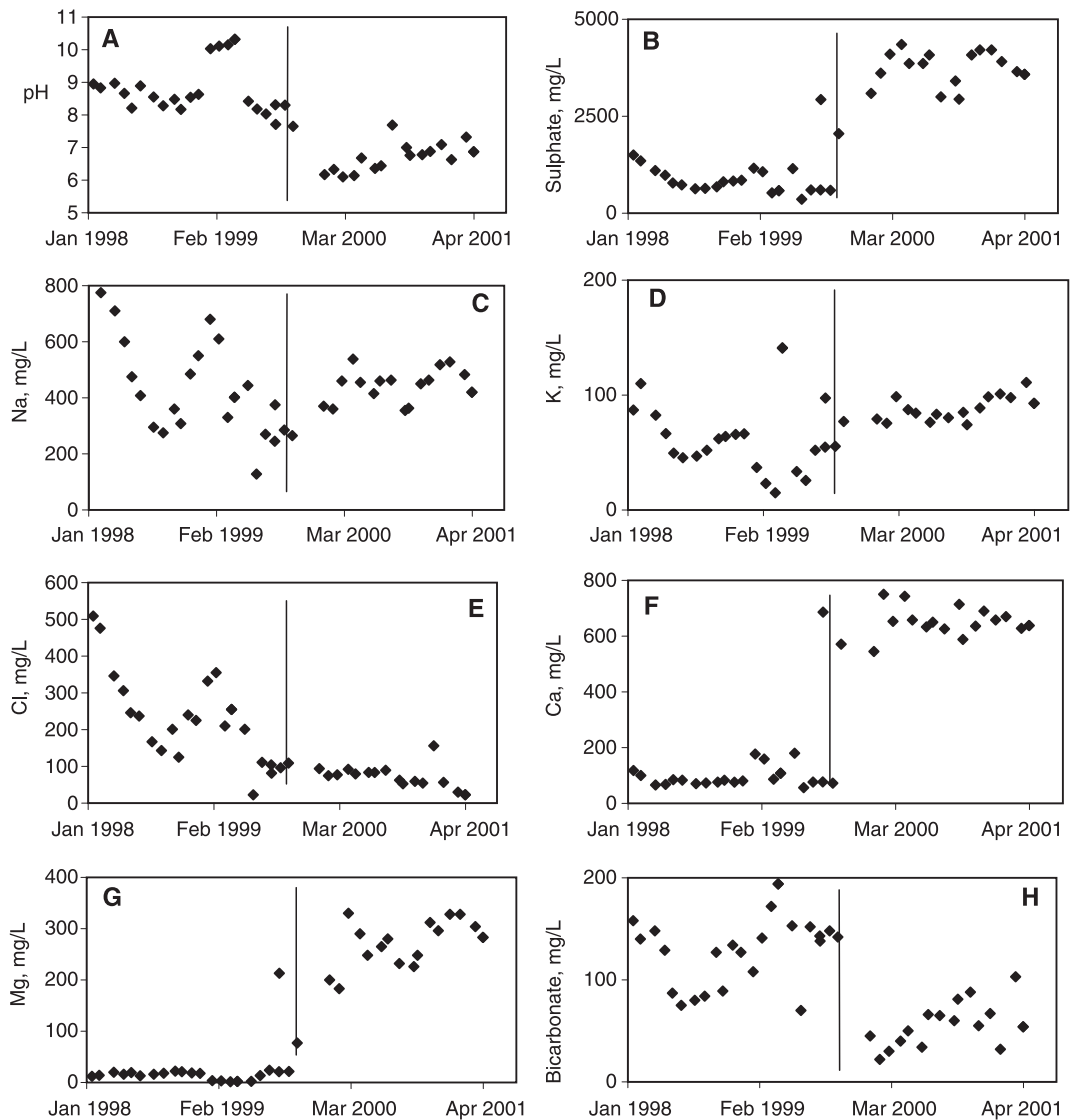


Fig. 2. Time series geochemical plots of mixed tailings water major ion compositions over the transition to pressure–oxidation in mid-1999 (see text). Approximate time of transition is indicated with a vertical bar on each graph.

had a short residence time in the decant pond (on a scale of days).

#### 4.1. Water chemistry

Decant water composition was monitored regularly as part of the dam monitoring programme, and this provides an important indicator of chemical changes throughout the processing system. Chemical variations with time from early 1998 to early 2001 are examined in this study through change to pressure–oxidation in mid-1999. Chemical analyses were conducted by Chemsearch (University of Otago Chemistry Department), an internationally accredited laboratory. Techniques and detection limits are outlined by Craw (2000). Detection limits for major ions are less than 1 mg/l, and uncertainties are contained within the size of the symbols on all graphs. Iron and copper were determined by standard atomic absorption spectrometry. Arsenic analyses were conducted using graphite furnace atomic absorption spectrometry and/or standard atomic absorption spectrometry. Uncertainties in metal concentrations are contained within the plotted symbols on the diagrams below.

Graphical summaries of chemical changes with time over the transition to pressure–oxidation are shown in Figs. 2 and 4. The variability of mixed tailings of the dam water chemistry before pressure–oxidation began is partly due to temporary discharges of tailings into a separate dam (Craw et al., 2002), allowing dilution of the mixed tailings decant pond to occur. The pH of the decant water dropped suddenly as soon as pressure–oxidation began (Fig. 2A), and remained steady at about 6. Dissolved sulphate concentrations climbed steadily since the mine opened in 1990. The climb in sulphate content accelerated with the onset of pressure–oxidation and active sulphate production in the autoclave (Fig. 1), causing levels to exceed 4000 mg/l (Fig. 2B).

Dissolved sodium in the decant water has been variable since 1998 (Fig. 2C), with a general decline before pressure–oxidation was commissioned. With the onset of pressure–oxidation, the sodium content of the decant water increased again. Potassium and chloride concentration variations mirror those of sodium (Fig. 2D,E). Calcium and magnesium concentrations were low before pressure–oxidation, but rose steeply after pressure–oxidation began (Fig. 2F,G).

Bicarbonate concentration shows a substantial dip in 1998, as for Na, K, and Cl, but a subsequent rise was interrupted by a sudden fall when pressure–oxidation began (Fig. 2H).

Decant water iron content was generally low and consistent before pressure–oxidation (Fig. 3A). With the onset of pressure–oxidation, the iron content of the decant water rose dramatically (Fig. 3A). Arsenic concentrations in the decant water were variable but at times high (>10 mg/l) before pressure–oxidation commenced, but subsequently decreased substantially to <1 mg/l (Fig. 3B). Likewise, dissolved copper decreased with the onset of pressure–oxidation although data are more variable than for As and more sparse as the waters were analysed for Cu less frequently (Fig. 3C).

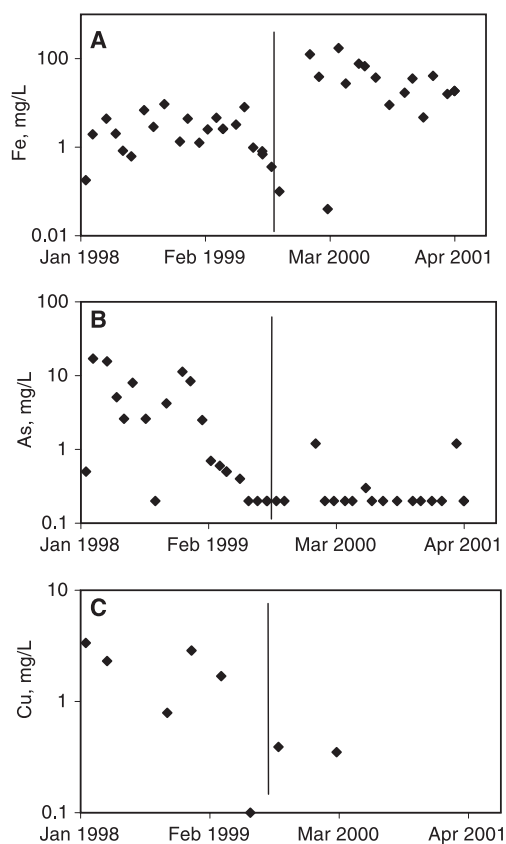


Fig. 3. Time series geochemical plots of mixed tailings water metal compositions over the transition to pressure–oxidation in mid-1999 (see text). Approximate time of transition is indicated with a vertical bar on each graph.

#### 4.2. Variation of pH with time

Decant pond water (pH = 6) sampled in November 1999 and kept in a plastic bottle for 3 months was noted to have pH of 3.6 when remeasured. The water was clear when sampled, but was brown in colour when re-examined in March 2000. In order to replicate these phenomena and to determine if the phenomena were peculiar to initiation of pressure–oxidation only, an additional sample of decant pond water was taken in April 2000. The sample was kept in a dark room at 18–20 °C, and the pH was measured at irregular intervals over the subsequent 6 weeks (Fig. 4).

The pH of the decant water showed a steady but nonlinear decrease over the experimental time, from an initial value of 6.1 to 3.8. The rate of pH change accelerated after about 1 month and then slowed once the pH near 4 was reached (Fig. 4). Brown pigmentation appeared after a few days and became progressively deeper in colour with time. Some of the brown material settled to the floor of the container as a sediment layer. This sediment was removed in June and analysed by XRD to determine if any crystalline material had formed. The sediment largely consists of gypsum crystals, up to 2 mm long, with interspersed amorphous brown particulate matter presumed to be iron oxyhydroxide. Microprobe examination con-

firmed a high Fe content, but the material was intimately intergrown with gypsum and detailed analysis was not possible. This precipitate strongly resembles the scales which form in the return water pipe which recycle water from the decant pond to the plant (above; Fig. 1).

### 5. Tailings

#### 5.1. Description

Tailings in the mixed tailing impoundment are essentially fan and lake sediments deposited downstream of discharge points which are rotated around the dam perimeter. The tailings are sandy with a substantial silt and mud component, and dewater rapidly to leave a firm open-textured sediment with about 50% pore space occupied by water (porosity determined by weight loss on drying; Craw et al., 1999). Finer grained layers deposited distally from the discharge points retain their water longer and remain soft and geliform after burial. Sedimentary layering is formed by discontinuous discharge from the range of points around the dam. Layers are typically 2–10 cm thick, and are defined by grain size variations. Microlaminations on the millimetre scale occur within these sedimentary layers.

Four holes were dug with spades in the tailings in April 2000, on a beach about 50 m from the edge of the decant pond, in tailings which were firm enough to support the weight of a person. The deepest hole was just over 1 m below surface, and digging stopped at this depth because water filled the base of the hole. The hole depths permitted sampling of tailings ca. 2 months old (estimated from normal deposition rates), and did not penetrate back to the onset of pressure–oxidation. Samples of water-saturated soft layers were taken, where present, for extraction of pore water by centrifuge.

The mineralogical makeup of the different sedimentary layers is essentially the same; they differ only in grain size. The tailings are dominated by quartz, feldspar, muscovite, and chlorite, the principal constituents of the schist host rock. In addition, clean monomineralic calcite detrital grains form about 5% of the tailings; this may be excess limestone from plant. This calcite is petrographically different from

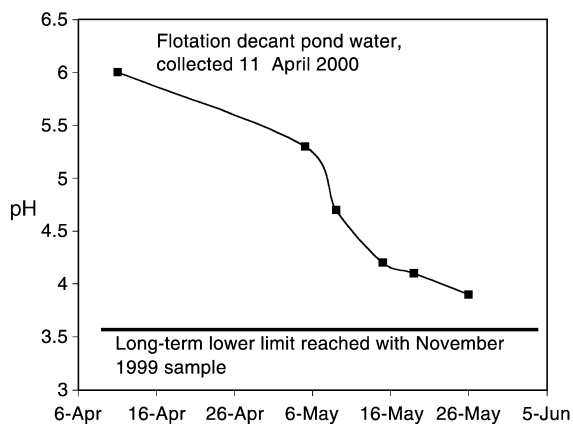


Fig. 4. Variation of pH in a sample of decant pond water (11 April 2000) kept in a dark laboratory for 6 weeks. The pH was measured at irregular intervals. The pH decreased at variable rates towards 3.6, the long-term lower limit which was measured after 3 months in a separate sample obtained in November 1999.

most schist calcite, which is predominantly finer grained and intergrown with other minerals.

Autoclave discharge material is difficult to identify in the tailings, but it appears to occur as scattered yellow brown composite grains with a smudgy appearance. These grains mainly consist of anhydrite, but smudgy brown opaque portions of some grains with elevated As (semiquantitative microprobe examination) are probably amorphous Fe arsenate. These grains have sharp margins and show no signs of in situ alteration. Some anhydrite/Fe arsenate composite grains have overgrowths of prismatic gypsum crystal clusters. The gypsum could be formed by precipitation from solution, or mineralogical transformation from anhydrite; textural observations are ambiguous.

Opaque minerals (incident light microscopy) in the tailings are pyrite, arsenopyrite, and rutile. These form <<1% of the tailings and occur as scattered individual grains and as inclusions in silicates. The sulphides show no sign of alteration before or after deposition, and are assumed to be from the flotation tailing portion of the circuit (Fig. 1), not the autoclave.

### 5.2. Pore water chemistry

In situ pore water pH was measured wherever sediment was sufficiently wet to permit reproducible measurements. In situ pH in the tailings ranged from 6.5 to 7.5, with most values near pH 7. Variation of up to 0.5 pH unit occurs between samples in close proximity (within 10 cm).

Pore waters extracted from samples by centrifuge were analysed for arsenic and copper, the metals most likely to be mobile in the tailings (Craw and Nelson, 2000). Extracted waters were analysed both with and without filtration (0.45 µm). The former measurement yields total metal content including metals in suspended solids. The filtered water analyses give an indication of dissolved metal concentrations, although even finer particles may exist than are extracted by the filter. The results show that total metal contents are all well below 1 mg/l, and dissolved metal contents are about a tenth of the total metal contents for each metal analysed. It is clear from the data set that the pore waters contain negligible quantities of dissolved arsenic and copper. The metal loads in the

pore waters are similar to those measured in decant pond waters after pressure–oxidation began (Fig. 3B,C).

## 6. Dam discharge water

### 6.1. Description

The mixed tailing dam is a very large structure approximately 1 km across and nearly 100 m high. It consists of disaggregated schist waste rock from the various excavations in the Macraes area. The upstream facing is relatively clay-rich and less permeable than the main dam structure, and includes permeable quartz gravel zones which form chimney drains to channel water to the base of the dam (Craw and Nelson, 2000). Decant pond water and fluid from dewatering tailings immediately beneath the decant pond move into the dam structure and are captured by the chimney drains or flow along the base of the dam on the schist basement surface. In addition, surface and ground water flow through the dam structure and mix with tailing waters. All dam waters consist of at least 50% tailing water and the rest is natural water, and this proportion has been variable over time (Craw and Nelson, 2000).

All dam waters are ultimately captured at a schist bedrock depression, Sump B, at the toe of the dam, from where they are recycled back to the processing plant (Fig. 1). Dam discharge waters in the chimney drains arrive at Sump B, mainly via pipes beneath the dam, at a rate of 11–12 l/s. Subsurface water flow passes through schist aggregate for most of its travel path before being captured by a pipe and channeled to Sump B. Consequently, subsurface waters have a different chemistry from that of chimney drain waters that have had less chance to interact with the schist aggregate (Craw, 2000).

### 6.2. Water chemistry and comparison to decant pond water

Dissolved sulphate concentrations in Sump B waters have remained approximately constant at 1000–1500 mg/l throughout the transition to pressure–oxidation (Fig. 5A). The subsurface waters have a higher sulphate than the chimney drain

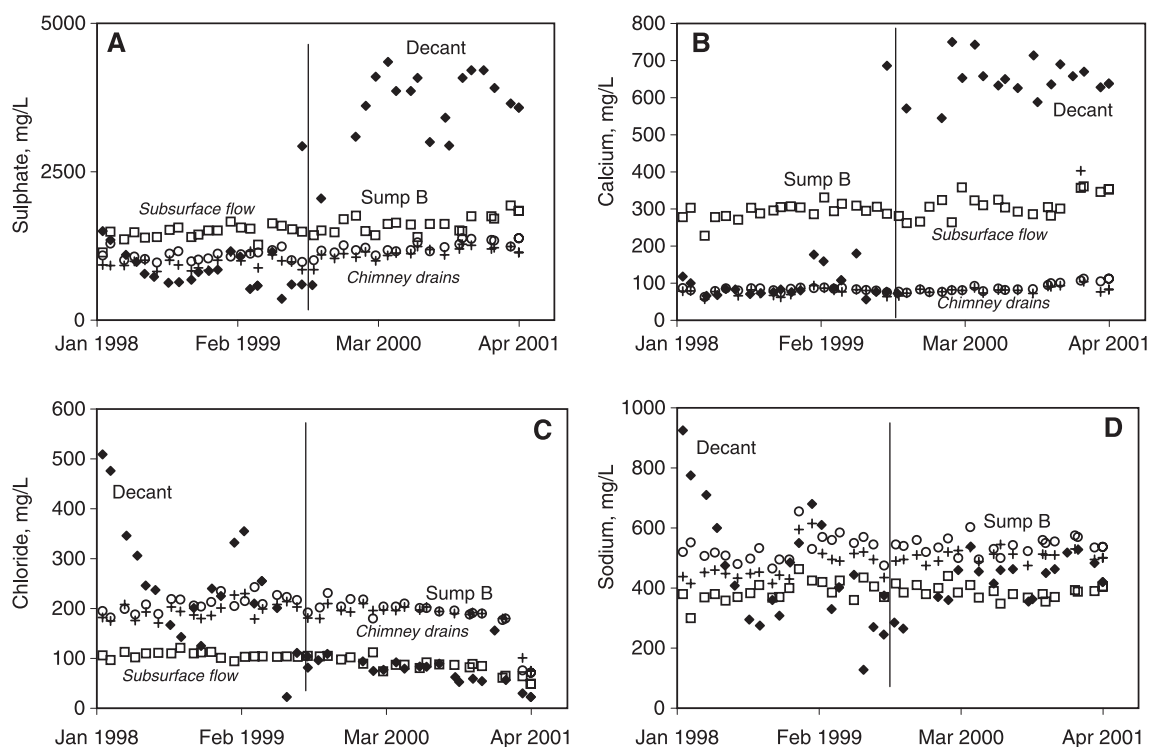


Fig. 5. Time series geochemical plots of dam discharge water major ion compositions at Sump B over the transition to pressure-oxidation in 1999 (see text). Approximate time of transition is indicated with a vertical bar on each graph. Subsurface water flow beneath the dam, as captured at Sump B, is shown with open squares, and chimney drain waters captured at sump B are shown with open circles and + symbols. Decant water compositions over the same time period (filled diamonds; Fig. 2) are shown for comparison.

waters (Fig. 5A) because of the water-rock interaction within the dam, mainly involving pyrite oxidation in weakly mineralised rock (Craw, 2000). Similarly, calcium concentrations have remained approximately constant in Sump B waters through the pressure-oxidation transition (Fig. 5B). Subsurface flowing waters have higher Ca due to dissolution of calcite in the schist aggregate of the dam (Craw, 2000). Other elements show similar patterns to those of calcium and sulphate, and only chloride (Fig. 5C) and sodium (Fig. 5D) are included here for reference.

Dissolved sulphate is the most prominent species from tailings which reaches Sump B and the amount of dissolved sulphate increased slowly but steadily from the time the mine opened in 1989 (Craw and Nelson, 2000). The dissolved sulphate was a useful indicator of the proportion of tailings water in the discharging water, and sulphate levels in chimney

drains were between 0.5 and 0.9 of the decant water sulphate levels. With the onset of pressure-oxidation in late 1999, this relationship broke down. Instead, while the decant pond waters increased dramatically in sulphate content, the Sump B waters leveled out and have remained at 1998 levels, between 1000 and 1200 ppm (Fig. 5A). Calcium concentrations show a similar pattern (Fig. 5B).

## 7. Discussion

### 7.1. Saturation indices

Saturation index is the ratio of products of the concentrations (activities) of dissolved species divided by the solubility product (Langmuir, 1997). This is normally expressed logarithmically. For this study, the software package AQUACHEM (incorporating

PHREEQC; Parkhurst, 1995) was used for calculation of saturation indices.

The saturation index for gypsum in decant waters before pressure–oxidation was consistently near 1 (Fig. 6A). This saturation index rose immediately after pressure–oxidation was started, and the decant waters have since remained mildly supersaturated with respect to gypsum (Fig. 6A). The decant waters are also nearly saturated with respect to anhydrite (Fig. 6B). Saturation indices for carbonate minerals show opposite trends to that of the gypsum index. Decant waters were supersaturated with respect to both calcite and dolomite before pressure–oxidation (Fig. 6C,D) by substantial amounts (in excess of 10 times saturation at times). This supersaturation ceased immediately when pressure–oxidation began, and the decant waters became undersaturated with respect to carbonates (Fig. 6C,D). This decrease in carbonate saturation is almost certainly due to the decrease in pH of decant waters that accompanied pressure–oxidation (Fig. 2A).

The constancy of calcium and sulphate concentrations at Sump B (Fig. 5A,B) is reflected in the gypsum saturation indices for Sump B waters (Fig. 6A). Only subsurface waters are plotted for Sump B in Fig. 6A because these are more concentrated than the chimney drain waters. The subsurface waters remain undersaturated with respect to gypsum through the transition to pressure–oxidation (Fig. 6A). Sump B subsurface waters are marginally undersaturated with respect to calcite, and undersaturated with respect to dolomite (Fig. 6C,D).

### 7.2. Calcium sulphate deposition

Pipes transmitting pressure–oxidation discharge from the plant to the decant pond become scaled with gypsum ( $\text{CaSO}_4 \cdot 2\text{H}_2\text{O}$ ) and locally with bassanite ( $\text{CaSO}_4 \cdot 0.5\text{H}_2\text{O}$ ) (Fig. 1). This scaling is due to supersaturation of the discharge with gypsum, the hydrated form of anhydrite, a major component of the discharge. Similar scaling by gypsum and iron oxyhydroxide occurs in the return water pipes as decant water is recycled (Fig. 1). The saturation index of decant water with respect to gypsum (above; Fig. 6A) confirms the widespread supersaturation of gypsum in plant waters and explains the extensive scaling.

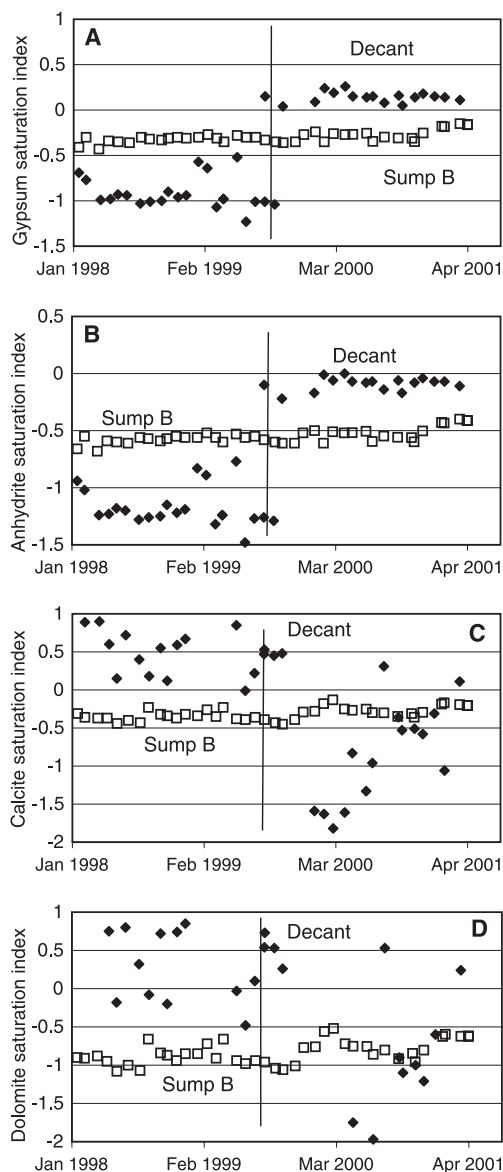


Fig. 6. Saturation indices for gypsum, calcite, and dolomite in the decant pond and the subsurface flow discharging at Sump B. The saturation index for a mineral is the logarithm of the ratio of observed concentrations of dissolved species to the solubility product (see text). Saturated solutions have SI of zero. The saturation indices in this diagram were calculated using program PHREEQC (Parkhurst, 1995). Approximate time of transition to pressure oxidation is indicated with a vertical bar on each graph.

Sump B Ca and sulphate concentrations changed little over the transition to pressure–oxidation, whereas in the decant pond, these components rose steadily

(Fig. 5A,B). The degree of saturation with respect to gypsum changed little in Sump B waters into the year 2000, while the decant pond became supersaturated with respect to gypsum (Fig. 6A). These observations suggest that gypsum was being deposited in the dam structure as the tailing waters percolated through the dam. This suggestion is in accord with observations of gypsum scaling in the return water pipes recycling water from the decant pond to the plant. Gypsum deposition in the dam could add scale to the dam discharge pipes, and ultimately seal the water discharge pathways through the dam. It is possible to estimate the mass of gypsum,  $M_{\text{gypsum}}$ , that was being deposited from the dam discharge waters using the following equation:

$$M_{\text{gypsum}} = 1.7[C_{\text{sulphate,decant}} - (C_{\text{sulphate,SumpB}} / X_{\text{decant,SumpB}})]Q_{\text{SumpB}} \quad (1)$$

where  $C_{\text{sulphate,decant}}$  is the decant pond sulphate content (Fig. 3B),  $C_{\text{sulphate,SumpB}}$  is the Sump B sulphate content (Fig. 5A) which is corrected for the proportion of decant water in the chimney drain water ( $X_{\text{decant,SumpB}}$ ; between 0.5 and 0.9), and  $Q_{\text{SumpB}}$  is the rate of water discharge at Sump B (11–12 l/s). The results are strongly dependent on the value chosen for degree of dilution of chimney drain water. These calculations suggest that between 1 and 4 tonnes of gypsum per day were being deposited in the dam structure.

A similar calculation can be made using differences in Ca concentrations between decant pond and chimney drains. The calcium results for October 1999 are identical to the same calculation using sulphate. However at later dates, the correspondence is much poorer with the Ca calculation giving consistently lower estimates of gypsum precipitation mass than the sulphate calculation. The differences between decant water Ca and chimney drain Ca are smaller than sulphate difference for these waters. This discrepancy may be due to dissolution of calcite by chimney drain waters as they pass through the tailings into the dam structure (Craw, 2000). The lower pH of decant water since pressure–oxidation began (pH=ca. 6) will have caused calcite to dissolve at a faster rate than when the decant water pH was >8.

### 7.3. Oxidation of Fe(II)

Fe(II) is not stable in oxygenated surface waters in contact with the atmosphere, and it oxidizes to Fe(III). At near-neutral pH, the oxidation reaction releases 2 mol of hydrogen ions for each mole of iron oxidized (Lowson, 1982; Langmuir, 1997). Hence, this reaction is a potent source of acidity in the decant water. Since acidification of the decant water is accompanied by formation of amorphous brown iron oxyhydroxide (=Fe(OH)<sub>3</sub>?), it is likely that this reaction is the main, possibly only, driving force for the observed acidification of the decant water. If so, maximum acid generation can be estimated from the amount of dissolved Fe(II) (above). The high sulphate content of the mine waters results in ca. half the Fe(II) forming dissolved ferrous sulphate complex (as determined from PHREEQC), but this complex will progressively decompose as Fe(II) oxidizes. Decant waters typically contain about 0.001 mol/l of Fe(II), and this can be up to 0.003 mol/l (April 2000). Hence, typically about 0.002 mol/l hydrogen ions will be ultimately generated, and up to 0.006 mol/l hydrogen ions in April 2000 decant water. This implies that the pH of the April 2000 decant water could theoretically drop to 2.2.

Despite the predicted low of pH near 2 for decant pond water, the rate of pH drop as measured in the laboratory slowed at pH of 3.9 (Fig. 4). The rate of oxidation of Fe(II) is therefore relevant to decant water acidification. Oxidation of Fe(II) is dependent on two main factors: access of oxygen to the ferrous iron and the rate of the oxidation reaction. Oxygen is only sparingly soluble in water (0.00026 mol/l; Langmuir, 1997), and diffuses slowly through that water (Langmuir, 1997; Elberling and Damgaard, 2001). Hence, in the laboratory situation, oxygen diffusion limits the rate of Fe(II) oxidation. Physical mixing and aeration of decant water occur by wind activity and water recycling, so oxygen access is enhanced in the field situation.

Once oxygen has diffused to Fe(II) ions, the rate of oxidation affects the rate of generation of hydrogen ions and subsequent pH drop. This reaction rate is determinable from the empirical rate law for the oxidation reaction (Stumm and Morgan, 1981; Langmuir, 1997). This reaction rate is rapid (hours to days) at pH near 6 in contact with air but when the pH has

lowered to 4, atmospheric oxygen levels take years to oxidize the Fe(II) (Stumm and Morgan, 1981; Langmuir, 1997). Oxidation of Fe(II) in Macraes decant water results in lowering of pH to 4 over 40 days (Fig. 5), so the oxidation reaction becomes self-limiting on time scales less than years. At the theoretical lowest limit of pH 2.2 for the April 2000 decant water (above), the reaction rate would be about four orders of magnitude slower than that at pH 4 (Stumm and Morgan, 1981; Langmuir, 1997). Hence, the observed lower limit of pH observed in the decant water experiment (3.9; Fig. 5) is the practical lower limit for human time scales despite the theoretical potential for greater hydrogen ion generation estimated from the solution iron concentration (above).

#### 7.4. Controls on tailing pH

Tailings were discharged at pH near 6, and this rapidly evolved to 6.5 within 1 day. All tailings examined in sampling holes had  $\text{pH} > 6.5$ , including the youngest (shallowest) layers which have pH near 7 only a few days after deposition. Calcite is a common mineral in the tailings, as a significant component of the schist and as material added in the feed to neutralise acidity in the plant (above; Fig. 1) and this continues in the tailings dam. Calcite reaction opposes the trend to lower the pH shown by decant water separated from the tailing solids (Fig. 4). Hence, the pH of the tailings at any time was the result of two opposite trends: acidity from Fe(II) oxidation and calcite dissolution. The tailings contain ca. 5 wt.% calcite (above), so that 1000 g of tailings can neutralise 0.5 mol of acidity. Tailings have a porosity of ca. 50% on deposition, and tailing water which fills that porosity has up to 0.006 mol/l of acidity generated by Fe(II) oxidation (above). Hence, there is ca. 100 times excess neutralisation capacity in the tailings than that required to offset acidification by oxidation of dissolved Fe(II).

The rise in pH immediately on deposition caused the pore waters to trend towards calcite equilibrium. Calcite dissolution reactions and rates near calcite equilibrium are slower and more complex than in lower pH solutions (Berner, 1978; Langmuir, 1997; Al et al., 2000). Hence, rise in pH beyond 7 will be a slow process, but is inevitable because of the high calcite content (ca. 5%) of the tailings. A geochemical

model (Fig. 7) can be constructed to show possible pH evolution of pore waters in mixed tailings. Two decant pond compositions (January and April 2000) were selected as representative of pore waters that were buried with the tailings after pressure–oxidation began. Calcite was added to these waters numerically using program PHREEQC. The pH rises progressively as more calcite dissolves (Fig. 7). Calcite saturation is reached at a pH of about 7, the observed year 2000 tailings pore water pH. Further calcite dissolution in the model raises the pH to higher levels, and results in calcite supersaturation (upper right portions of the curves in Fig. 7). Typical decant pond waters before pressure–oxidation are plotted as black squares in Fig. 7, showing that calcite supersaturation was the norm, and calcite saturation indices as high as 0.7 were reached. Similar levels of calcite supersatu-

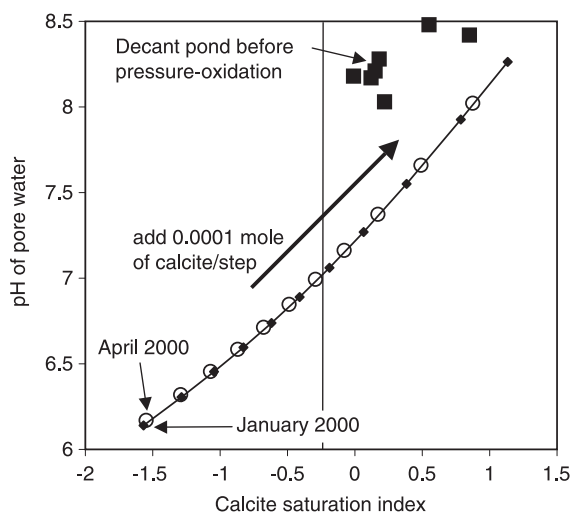


Fig. 7. Geochemical model showing possible pH evolution of tailing waters in the mixed tailings. Two decant pond compositions (January and April 2000) were selected as representative of tailing waters which were buried with the tailings after pressure–oxidation began. These are plotted at the low pH end of the model curves (lower left) and are undersaturated with respect to calcite, as determined with program PHREEQC. Calcite was added to these waters numerically, using program PHREEQC. The pH rises progressively as more calcite dissolves. Calcite saturation is reached at a pH of about 7. Further calcite dissolution raises the pH to higher levels, and results in calcite supersaturation (upper right portions of the curves). Typical decant pond waters before pressure–oxidation are plotted as black squares, showing that calcite supersaturation was the norm, and calcite saturation indices as high as 0.7 were reached. Similar levels of calcite supersaturation in present tailing waters would result in pH of 7.5–8.

ration in pressure–oxidation tailing pore waters in year 2000 tailings would result in pore water pH of 7.5–8 (Fig. 7). The pH of decant pond water was 7.5 in early 2002 when use of the tailings impoundment was discontinued, but these tailings are no longer accessible to test this hypothesis.

### 7.5. Long-term dissolved arsenic concentrations

The tailings contain arsenic in two forms: solid Fe arsenate from the autoclave and dissolved As. The total solid As content of the tailings is <1%. The dissolved arsenic content of tailings water in the decant pond, and in pore waters in contact with the As-bearing sediments, is very low (<1 mg/l; Fig. 3B).

The dissolved arsenic content of tailing waters from pressure–oxidation is distinctly lower than that prevailing before pressure–oxidation. The initially high As was due to oxidation and dissolution of arsenopyrite in the processing plant (Craw and Pacheco, 2002). Once pressure–oxidation began, arsenopyrite was completely decomposed in the autoclave (above) and the discharge contained As in a solid form that may be less soluble than arsenopyrite. The level of dissolved As remained low, probably because of adsorption of As to fine-grained Fe(III) oxyhydroxides (Roddick-Lanzilotta et al., 2002). The distribution coefficient for this adsorption,  $K_d = 10^5$ – $10^6$  (Roddick-Lanzilotta et al., 2002; Smedley and Kinniburgh, 2002), implies that adsorbed As amounts will be several orders of magnitude higher than dissolved arsenic. Progressive precipitation of Fe(III) oxyhydroxides from tailing waters due to oxidation of dissolved Fe(II) (above) will ensure that the surface area for this adsorption remains high.

Experimental work on the solubility of Fe arsenates has shown that solubility is affected by the Fe/As ratio, the amount of sulphur in the structure, and the pH of the solution (Krause and Ettl, 1989). Fe arsenates with high Fe/As ratios and structural sulphate are all amorphous, as in the Macraes autoclave discharge material (above), and their mineralogical identity is unknown. The experimental data for this type of material imply that As solubility should be between 0.2 and 2 ppm (Krause and Ettl, 1989). This is higher than actually observed (Fig. 3B), so presumably Macraes tailings sampled thus far have not reached equilibrium. Hence, dissolved As content

of tailing waters can be expected to rise by at least an order of magnitude but As levels will still be lower than historic As contents of Macraes mine waters (Fig. 3B).

Adsorption of As from discharge waters occurred onto perpetually regenerating Fe(III) oxyhydroxide at Sump B, keeping dissolved As very low in discharge waters, which take about 12 days to follow the ca. 1 km flow path through the dam, or ca. 80 m/day (Roddick-Lanzilotta et al., 2002). Retardation of As by adsorption is related to the distribution coefficient,  $K_d$ , for arsenic between solid and solution by:

$$v_{\text{water}}/v_{\text{arsenic}} = 1 + (\rho_b/\phi)K_d \quad (2)$$

where  $v_{\text{water}}$  and  $v_{\text{arsenic}}$  are specific discharges (Darcy velocities) for discharge water and an arsenic geochemical front, respectively; and  $\rho_b$  is the bulk density and  $\phi$  the porosity of the medium through which the water passes (Freeze and Cherry, 1979; Langmuir, 1997). The ratio of  $\rho_b/\phi$  is estimated to be about 6–8 for the Macraes dam, based on observations of dam materials. Hence, appreciable dissolved As is expected to move through the dam at ca. one millionth the rate that water does, or 30 mm/year. This calculation assumes that the water pathway is coated with Fe(III) oxyhydroxide, and that no new Fe(III) oxyhydroxide is added chemically. The former assumption is reasonable, based on observations at Sump B and chemical considerations (above). The latter assumption is probably not correct as new Fe(III) oxyhydroxide is constantly being deposited, and the As specific discharge may be even slower than 30 mm/year.

## 8. Conclusions

Pressure–oxidation technology imposed on arsenopyrite- and pyrite-bearing gold ore results in substantial changes in mineralogy of mine processing plant discharge material. The principle new minerals are anhydrite, jarosite, and amorphous Fe arsenates. The change from traditional cyanidation to pressure–oxidation at the Macraes Mine resulted in major chemical changes in the mine tailings system, as summarised in Fig. 8. Dissolved sulphate in the tailing waters rose steadily, and these waters were saturated with respect to gypsum but undersaturated with

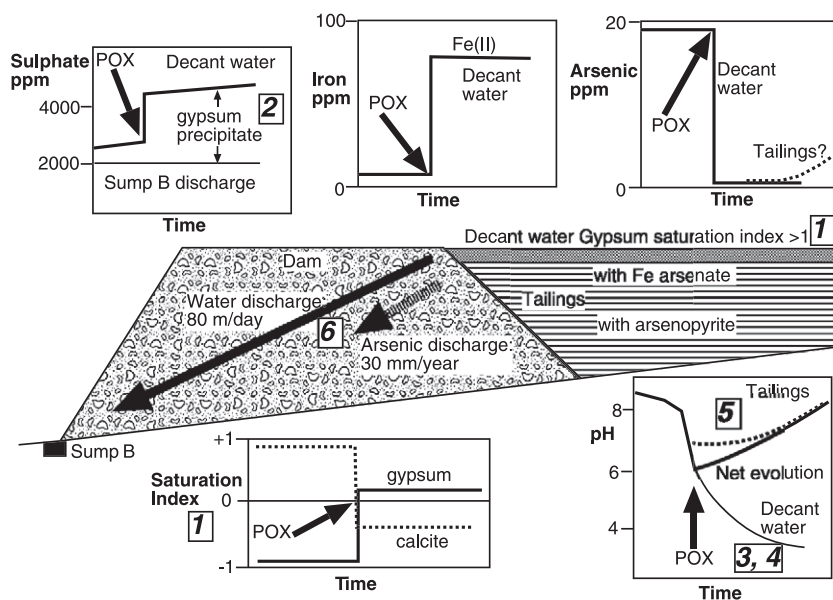


Fig. 8. Cartoon summarising the principal chemical changes which have occurred in the Macraes tailings complex in the transition to pressure–oxidation (POX), as outlined in the text. A sketch of the tailing complex (centre) shows the principal relevant features and the various waters described in the text. Numbers in boxes in the cartoon refer to equations in the text relevant to the depicted chemical changes.

respect to calcite. Waters discharging from the tailing dam showed negligible change in dissolved sulphate because of precipitation of gypsum (1–4 tonnes/day) as cement within the dam structure. Dissolved iron in tailing waters rose with the onset of pressure–oxidation, and this iron was predominantly Fe(II). Oxidation of Fe(II) in tailing water removed from the tailing solids resulted in the lowering of pH over time down to ca. pH 4. A theoretical lower limit of ca. pH 2 will not be reached on human time scales. Tailings contain ca. 5 wt.% calcite, and this calcite neutralised acid generated by oxidation of Fe(II). Further dissolution of calcite resulted in evolution of tailing pH to progressively more alkaline pH, and this may continue to ca. pH 8. Dissolved arsenic decreased in pressure–oxidation discharge waters compared to waters from the traditional cyanidation process, because the Fe arsenates are less soluble than arsenopyrite in the processing plant. Dissolved arsenic may rise slowly in the future, but arsenic discharge from the tailing dam will remain at low levels because arsenic is readily adsorbed onto Fe(III) oxyhydroxide precipitates. These Fe(III) oxyhydroxide precipitates are constantly being added to the discharge system, providing additional adsorption sites. A plume of

dissolved arsenic could move through the dam at ca. 30 mm/year, to emerge at Sump B in >30 000 years.

## Acknowledgements

This study was financed by the New Zealand Foundation for Research, Science and Technology, with additional support from GRD Macraes. The work would not have been possible without the enthusiasm and logistical support of GRD Macraes personnel at the Macraes site, particularly D. Wilson, Q. Johnston, M. Cadzow, S. LaBrooy, and A. Marin. Technical assistance from D. Chappell and B. Grant facilitated field and laboratory work.

## References

- Al, T.A., Martin, C.J., Blowes, D.W., 2000. Carbonate–mineral/water interactions in sulfide-rich mine tailings. *Geochim. Cosmochim. Acta* 64, 3933–3948.
- Berner, R.A., 1978. Rate control of mineral dissolution under earth surface conditions. *Am. J. Sci.* 278, 1235–1252.
- Craw, D., 2000. Water–rock interaction and acid neutralization in a

- large schist debris dam, Otago, New Zealand. *Chem. Geol.* 171, 17–32.
- Craw, D., Nelson, M., 2000. Geochemical signatures of discharge waters, Macraes mine flotation tailings, east Otago, New Zealand. *N.Z. J. Mar. Freshw. Res.* 34, 597–613.
- Craw, D., Pacheco, L., 2002. Mobilisation and bioavailability of arsenic around mesothermal gold deposits in a semiarid environment, Otago, New Zealand. *Sci. World J.* 2, 308–319.
- Craw, D., Chappell, D., Nelson, M., Walrond, M., 1999. Consolidation and incipient oxidation of alkaline arsenopyrite-bearing mine tailings, Macraes Mine, New Zealand. *Appl. Geochem.* 14, 485–498.
- Craw, D., Koons, P.O., Chappell, D.A., 2002. Arsenic distribution during formation and capping of an oxidized sulphidic mine soil, Macraes mine, New Zealand. *J. Geochem. Explor.* 76, 13–29.
- Elberling, B., Damgaard, L.R., 2001. Microscale measurements of oxygen diffusion and consumption in subaqueous sulfide tailings. *Geochim. Cosmochim. Acta* 65, 1897–1905.
- Freeze, R.A., Cherry, J.A., 1979. *Groundwater*. Prentice-Hall, Englewood Cliffs, NJ.
- Krause, E., Ettel, V.A., 1989. Solubilities and stabilities of ferric arsenate compounds. *Hydrometallurgy* 22, 311–337.
- Langmuir, D., 1997. *Aqueous Environmental Geochemistry*. Prentice-Hall, Upper Saddle River, NJ, USA. 600 pp.
- Lowson, R.T., 1982. Aqueous oxidation of pyrite by molecular oxygen. *Chem. Rev.* 82, 461–497.
- McKeag, S.A., Craw, D., Norris, R.J., 1989. Origin and deposition of a graphitic schist-hosted metamorphogenic Au–W deposit, Macraes, East Otago, New Zealand. *Miner. Depos.* 24, 124–131.
- Parkhurst, D.L., 1995. Users guide to PHREEQC. A computer program for speciation, reaction-path, advective-transport, and inverse geochemical calculations. U.S. Geol. Surv. Water Res. Inv. Rep., 95–4227.
- Ritcey, G.M., 1989. Effluent treatment for environmental control. Tailings management: problems and solutions in the mining industry. *Process Metallurgy Report*, vol. 6. Elsevier, Amsterdam, pp. 411–574.
- Roddick-Lanzilotta, A.J., McQuillan, A.J., Craw, D., 2002. Infrared spectroscopic characterisation of arsenate(V) ion adsorption from mine waters, Macraes Mine, New Zealand. *Appl. Geochem.* 17, 445–454.
- Smedley, P.L., Kinniburgh, D.G., 2002. A review of the source, behaviour and distribution of arsenic in natural waters. *Appl. Geochem.* 17, 517–568.
- Stumm, W., Morgan, J.J., 1981. *Aquatic Chemistry*, 2nd ed. Wiley, New York. 780 pp.